

## A new anhydrous amphibole from the Eifel region, Germany: Description and crystal structure of obertiite, $\text{NaNa}_2(\text{Mg}_3\text{Fe}^{3+}\text{Ti}^{4+})\text{Si}_8\text{O}_{22}\text{O}_2$

FRANK C. HAWTHORNE,<sup>1,\*</sup> MARK A. COOPER,<sup>1</sup> JOEL D. GRICE,<sup>2</sup> AND LUISA OTTOLINI<sup>3</sup>

<sup>1</sup>Department of Geological Sciences, University of Manitoba, Winnipeg, Manitoba R3T 2N2 Canada  
<sup>2</sup>Research Division, Canadian Museum of Nature, P.O. Box 3343, Station D, Ottawa, Ontario K1P 6P4, Canada  
<sup>3</sup>CNR Centro di Studio per la Cristallochimica e le Cristallografia, via Abbiategrasso 209, 27100 Pavia, Italy

### ABSTRACT

Obertiite is a new amphibole species from Bellerberg, Laccher See district, Eifel, Germany. It occurs with tridymite, fluororichterite, hematite, rutile, aegirine-augite, kinoshitalite, and fluor-apatite in vugs in volcanic rocks, and crystallized from late-stage hydrothermal fluids associated with recent volcanism. Obertiite occurs as pale-pink elongated blades and divergent aggregates. It is brittle,  $H = 5$ ,  $D_{\text{calc}} = 3.16 \text{ g/cm}^3$ , has a colorless streak, vitreous luster, and does not fluoresce; it has perfect cleavage on {110} and conchoidal fracture. In plane-polarized light, obertiite is slightly pleochroic in shades of pink to red-orange;  $X \wedge a = 2^\circ$  (in  $\beta$  obtuse),  $Z = b$ ,  $Y \wedge c = 12^\circ$  (in  $\beta$  obtuse) with absorption  $X \sim Y \sim Z$ . It is biaxial negative,  $\alpha = 1.643(1)$ ,  $\beta = 1.657(1)$ ,  $\gamma = 1.670(3)$ ,  $2V_x = 81(1)^\circ$ , no dispersion visible. Obertiite is monoclinic, space group  $C2/m$ ,  $a = 9.776(2)$ ,  $b = 17.919(3)$ ,  $c = 5.292(1) \text{ \AA}$ ,  $\beta = 104.05(2)^\circ$ ,  $V = 899.3(3) \text{ \AA}^3$ ,  $Z = 2$ . The strongest ten X-ray diffraction lines in the powder pattern are [ $d(I,hkl)$ ]: 8.414(10,110), 2.705(7,331,151), 3.390(6,131), 4.467(5,040), 3.117(5,310), 2.531(5,202), 3.255(3,240), 2.577(3,061), 2.163(3,171,261), 4.013(2,111). Analysis by a combination of electron microprobe, SIMS, and crystal-structure refinement gives  $\text{SiO}_2$  54.53,  $\text{Al}_2\text{O}_3$  0.15,  $\text{TiO}_2$  7.75,  $\text{Fe}_2\text{O}_3$  2.61,  $\text{Mn}_2\text{O}_3$  3.27,  $\text{FeO}$  3.36,  $\text{ZnO}$  0.08,  $\text{MgO}$  14.13,  $\text{Li}_2\text{O}$  0.05,  $\text{CaO}$  0.52,  $\text{Na}_2\text{O}$  9.51,  $\text{K}_2\text{O}$  0.98, F 0.55,  $\text{H}_2\text{O}$  0.20, O  $\equiv$  F  $-0.23$ , Ni, Cr, V, Cl not detected, sum 97.46 wt%. The formula unit, calculated on the basis of 24(O,OH,F) is  $(\text{K}_{0.18}\text{Na}_{0.84})(\text{Na}_{1.86}\text{Ca}_{0.08}\text{Fe}^{2+}_{0.06})(\text{Mg}_{3.09}\text{Zn}_{0.01}\text{Li}_{0.02}\text{Fe}^{3+}_{0.29}\text{Mn}^{2+}_{0.37}\text{Fe}^{2+}_{0.41}\text{Ti}^{4+}_{0.86}\text{Al}_{0.03})\text{Si}_{8.00}\text{O}_{22}[(\text{OH})_{0.20}\text{F}_{0.26}\text{O}_{1.54}]$ , and is close to the ideal end-member composition  $\text{Na Na}_2(\text{Mg}_3\text{Fe}^{3+}\text{Ti}^{4+})\text{Si}_8\text{O}_{22}\text{O}_2$ .

The crystal structure of obertiite was refined to an  $R$  index of 2.6% using  $\text{MoK}\alpha$  X-ray intensity data. The M1 site is split into two subsites along the **b** axis, M1 and M1A; the M1 site is occupied by Mg, and M1A is occupied predominantly by  $\text{Ti}^{4+}$  and  $\text{Mn}^{3+}$ ; M2 is occupied by Mg,  $\text{Fe}^{2+}$ , and  $\text{Fe}^{3+}$ , and M3 is occupied by Mg. Local bond-valence considerations suggest that  $\text{O}^{2-}$  at O3 is linked to  $\text{Ti}^{4+}\text{Mg}$  or  $\text{Mn}^{3+}\text{Mn}^{3+}$  at the adjacent M1 and/or M1A sites, and that OH or F at O3 is linked to MgMg at the adjacent M1 sites.

### INTRODUCTION

While browsing for amphiboles in vugs of the Laccher See district, Germany, we noted two types of acicular crystals (yellow and pink) that had previously been described as “amphibole” and “hornblende.” Examination of these crystals by structure refinement showed the pink crystals to be a new amphibole species of particular interest, as it is only the second (root) amphibole with oxygen as the dominant species at the O3 site. We name this amphibole obertiite in honor of Roberta Oberti of Pavia, Italy for her seminal contributions to our understanding of the crystal chemistry of the amphibole-group minerals. The species and name have been approved by the International Mineralogical Association Commission on New Minerals and Mineral Names. Holotype material is deposited at the Canadian Museum of Nature, Ottawa, Canada.

### OCCURRENCE

Obertiite occurs in vugs in volcanic rocks at the Bellerberg quarry, Laccher See district, Eifel region, Germany. A wide variety of recent (<500 000 years old) volcanic rocks occur in the Laccher See district. Cavities within the basaltic lava flows, dykes, and pyroclastites contain a wide variety of minerals as free-standing euhedral crystals (Hentschel 1975, 1977) that may have crystallized from late hydrothermal fluids or even gases. This material circulates widely among micromineral collectors.

Amphibole is known to occur in these cavities. As this is an unusual paragenesis for amphiboles, we examined and characterized the amphiboles from this area. Careful observation showed two distinct types of amphibole: pink and honey yellow. The pink amphibole (obertiite) is associated with tridymite, (colorless hexagonal plates), acicular yellow fluororichterite, hematite (brilliant rhombohedral tablets), rutile (as red needles and carpets of orange drusy crystals), aegirine-augite (colorless-to-green acicular crystals), kinoshitalite (brown micaceous aggregates), and fluorapatite (flesh-pink waxy equant crystals).

\*E-mail: frank\_hawthorne@umanitoba.ca

## PHYSICAL AND OPTICAL PROPERTIES

Obertiite is pale pink with a colorless streak and a vitreous luster; it shows no fluorescence under long-wave or short-wave ultraviolet light. Large crystals (up to  $10 \times 40 \times 200 \mu\text{m}$ ) always taper along their length and show anomalous optical properties; smaller crystals ( $< 100 \mu\text{m}$  long) are not tapered and show normal optical properties in transmitted light. Obertiite has perfect {110} cleavage, is brittle, has conchoidal fracture, and has a Mohs' hardness of 5. The calculated density is  $3.16 \text{ g/cm}^3$ .

A spindle stage was used to orient a crystal for refractive-index measurement and determination of  $2V$  by extinction curves. The optic orientation was determined by transferring the crystal from the spindle stage to a precession camera and determining the relative axial relations by X-ray diffraction. In transmitted light, obertiite is slightly pleochroic in shades of pink to red-orange;  $X \wedge a = 2^\circ$  (in  $\beta$  obtuse),  $Y \wedge c = 12^\circ$  (in  $\beta$  obtuse),  $Z = b$ ; absorption  $X \sim Y \sim Z$  and there is no visible dispersion. Obertiite is biaxial negative with indices of refraction  $\alpha = 1.643(1)$ ,  $\beta = 1.657(1)$ ,  $\gamma = 1.670(3)$  measured with gel-filtered Na light ( $\lambda = 589.9 \text{ nm}$ );  $2V_x = 81(1)$ ,  $2V_{\text{calc}} = 93^\circ$ .

## CHEMICAL COMPOSITION

Obertiite was analyzed by electron-microprobe using a Cameca SX-50 operating in the wavelength-dispersive mode with excitation voltage 15 kV, specimen current 20 nA, peak-count time of 20 s and background-count time of 10 s. The following standards and crystals were used for  $K\alpha$  X-ray lines: Si, Ca = tremolite, PET; Ti = hornblende, LiF; Fe = arfvedsonite, LiF; Mn = tephroite, LiF; Mg = tremolite, TAP; Na, Al = albite, TAP; K = orthoclase, PET; F = fluororiebeckite, TAP; Zn = willemite, LiF. Data reduction was done using the  $\phi(\rho Z)$  procedure of Pouchou and Pichoir (1984, 1985). The average of 10 analyses on a single grain is given in Table 1.

Ion-microprobe analysis was done on a Cameca IMS 4f. Due to the very small dimensions of the amphibole crystal, an O<sup>-</sup> primary beam  $\leq 5$  micrometers in diameter, corresponding to a beam current of  $\sim 3.5 \text{ nA}$ , was used. The sample was left in the ion-microprobe sample chamber to degas for two days, together with low-H standard amphiboles that were used in the calibration procedure. The energy-filtering technique was used to eliminate any possible molecular interference and to reduce matrix effects affecting light-element ionization. Secondary positive-ion currents were measured at masses 1 (H), 7(Li), and 30 (Si was used as the reference element) and corrected for isotopic abundances. The results were put on a quantitative basis using empirical calibration curves based on standard silicate samples. In particular, for H quantification we used a sample of tremolite (Hawthorne and Grundy 1976) ( $\text{SiO}_2 = 56.57 \text{ wt\%}$ ;  $\text{H}_2\text{O} = 1.46 \text{ wt\%}$ ), and the amphiboles DL-5 and DH belonging to the working curve for H in silicates (Ottolini et al. 1995). Li quantification was done according to the procedure of Ottolini et al. (1993) and corrections were made to account for residual matrix effects, due mainly to the different silica content between this amphibole and the standards used. The accuracy of H and Li analysis is estimated to be in the order of 10% relative.

The unit formula was calculated on the basis of  $24(\text{O}, \text{OH}, \text{F})$ . When calculating the unit formula of amphiboles character-

ized by SREF (site-scattering refinement) from microprobe data, we derive the  $\text{Fe}^{3+}/\text{Fe}^{2+}$  ratio from stereochemical criteria (Hawthorne 1983). When there is significant Mn present, we have usually assumed that Mn is in the divalent state (e.g., Hawthorne et al. 1993). However, the situation in obertiite is somewhat different as the O3 site is occupied predominantly by O<sup>2-</sup>. Hawthorne et al. (1995) described another amphibole, ungarettiite, in which O<sup>2-</sup> is dominant at the O3 site. In ungarettiite, the M1A site is occupied by Mn<sup>3+</sup>, and the unusual pattern of bond lengths (involving a very short bond to O3) is promoted by the Jahn-Teller distortion typical for the  $d^4$  electron configuration of Mn<sup>3+</sup>. As both Mn<sup>3+</sup> and Fe<sup>3+</sup> have the same cation radius (Shannon 1976) and the radii of Fe<sup>2+</sup> (0.78 Å) and Mn<sup>3+</sup> (0.83 Å) are fairly similar, it is not possible to distinguish between Fe<sup>3+</sup> and Mn<sup>3+</sup> in these circumstances. Thus we have calculated the unit formula for two possibilities: (1) all Mn as Mn<sup>2+</sup>; (2) all Mn as Mn<sup>3+</sup>, with the  $\text{Fe}^{3+}/\text{Fe}^{2+}$  ratio derived from stereochemical data. Both possibilities are shown in Table 1.

## X-RAY CRYSTALLOGRAPHY

The powder diffraction pattern was recorded from a small fragment on a Gandolfi camera with Fe-filtered CuK $\alpha$  X-radiation. Cell dimensions were refined from the corrected  $d$  values using the program Celref (Appleman and Evans 1973); the indexed powder pattern and refined cell dimensions are given in Table 2. Peak intensities reported in Table 2 are those calculated from the refined crystal structure; these values agree with the values estimated by eye from the darkening on the film.

**TABLE 1.** Electron- and ion-microprobe analysis\* (wt%) and unit formula (apfu) for obertiite

|                                |       |                  |       |
|--------------------------------|-------|------------------|-------|
| SiO <sub>2</sub>               | 54.53 | Si               | 8     |
| Al <sub>2</sub> O <sub>3</sub> | 0.15  | Al               | 0.03  |
| TiO <sub>2</sub>               | 7.75  | Ti               | 0.86  |
| Fe <sub>2</sub> O <sub>3</sub> | 2.61† | Fe <sup>3+</sup> | 0.29† |
| Mn <sub>2</sub> O <sub>3</sub> | 3.27† | Mn <sup>3+</sup> | 0.37† |
| FeO                            | 3.36† | Fe <sup>2+</sup> | 0.41† |
| MnO                            | 0.00† | Mn <sup>2+</sup> | 0.00† |
| ZnO                            | 0.08  | Zn               | 0.01  |
| MgO                            | 14.13 | Mg               | 3.09  |
| Li <sub>2</sub> O              | 0.05  | Li               | 0.03  |
| CaO                            | 0.52  | ΣC               | 5.06  |
| Na <sub>2</sub> O              | 9.51  |                  |       |
| K <sub>2</sub> O               | 0.98  | Fe <sup>2+</sup> | 0.06  |
| F                              | 0.55  | Ca               | 0.08  |
| H <sub>2</sub> O               | 0.2   | Na               | 1.86  |
| ≡ F                            | -0.23 | SB               | 2     |
|                                |       | Na               | 0.84  |
|                                |       | K                | 0.18  |
|                                |       | ΣA               | 1.02  |
|                                |       | OH               | 0.2   |
|                                |       | F                | 0.26  |
|                                |       | O                | 1.54  |
|                                |       | Σ                | 2     |

\* Average of 10 analyses on a single grain.

† Values assumed all Mn as Mn<sup>3+</sup> with  $\text{Fe}^{3+}/\text{Fe}^{2+}$  derived from stereochemical data.

‡ Values assumed all Mn as Mn<sup>2+</sup> with  $\text{Fe}^{3+}/\text{Fe}^{2+}$  derived from stereochemical data.

## X-ray data collection

A small optically homogeneous crystal was mounted on a Siemens *P4* automated four-circle diffractometer; reflections were aligned using MoK $\alpha$  X-radiation. The cell dimensions were determined by least-squares refinement of the setting angles, and the values are given in Table 3. A total of 1568 intensities was collected according to the procedures of Hawthorne and Groat (1985). The intensities were reduced to structure factors with the usual geometrical and absorption corrections, resulting in 1074 reflections, 630 of which are considered as observed ( $|F_o| > 5\sigma_F$ ).

**TABLE 2.** X-ray powder-diffraction data for obertiite

| $I_{\text{calc}}$ | $d_{\text{obs}}$ (Å) | $d_{\text{calc}}$ (Å) | $h k l$ |
|-------------------|----------------------|-----------------------|---------|
| 10                | 8.414                | 8.396                 | 1 1 0   |
| 5                 | 4.467                | 4.472                 | 0 4 0   |
| 2                 | 4.013                | 4.012                 | 1 1 1   |
| 2                 | 3.855                | 3.86                  | 1 3 1   |
| 6                 | 3.39                 | 3.388                 | 1 3 1   |
| 3                 | 3.255                | 3.257                 | 2 4 0   |
| 5                 | 3.117                | 3.121                 | 3 1 0   |
| 1                 | 2.942                | 2.953                 | 2 2 1   |
|                   |                      | 2.922                 | 1 5 1   |
| 1                 | 2.79                 | 2.799                 | 3 3 0   |
| 7                 | 2.705                | 2.716                 | 3 3 1   |
|                   |                      | 2.7                   | 1 5 1   |
| 3                 | 2.577                | 2.578                 | 0 6 1   |
| 5                 | 2.531                | 2.532                 | 2 0 2   |
| 2                 | 2.32                 | 2.321                 | 3 5 1   |
| 1                 | 2.269                | 2.268                 | 3 1 2   |
| 3                 | 2.163                | 2.171                 | 1 7 1   |
|                   |                      | 2.158                 | 2 6 1   |
| 2                 | 2.057                | 2.058                 | 2 0 2   |
| 1                 | 1.65                 | 1.65                  | 4 6 1   |
| 2                 | 1.58                 | 1.58                  | 1 5 3   |
| 2                 | 1.431                | 1.431                 | 6 6 1   |

Note:  $a = 9.805(4)$   $b = 17.89(1)$   $c = 5.294(2)$   $\beta = 104.14(4)$ .

## Structure refinement

All calculations were done with the SHELXTL PC(Plus) system of programs;  $R$  indices are of the form given in Table 3. The structure converged rapidly for an anisotropic-displacement model for all atoms. The M1 site showed extreme anisotropic displacement in the [010] direction. This was modeled by splitting the M1 site into two sites, M1 and M1A, with variable  $y$  coordinates, independently variable site-scattering values and identical (constrained) and variable anisotropic-displacement factors. Full-matrix refinement of all variables converged to an  $R$  index of 2.6%. Final positions and displacement parameters are listed in Table 4, selected interatomic distances are given in Table 5, and refined site-scattering values are given in Table 6; structure factors are listed in Table 7.<sup>1</sup>

## Site populations

The site populations were derived from consideration of the site-scattering refinement results, the unit formula calculated from the electron-microprobe and SIMS analyses, and the observed mean bond-lengths.

<sup>1</sup>For a copy of Table 7, document item AM-99-032, contact the Business Office of the Mineralogical Society of America (see inside front cover of recent issue) for price information. Deposit items may also be available on the American Mineralogist web site (<http://www.minsocam.org> or current web address).

**TABLE 3.** Miscellaneous data collection and refinement information for obertiite

|   |           |                                  |                        |
|---|-----------|----------------------------------|------------------------|
| $a$ (Å)   | 9.776(2)  | Crystal size ( $\mu\text{m}^3$ ) | 14 × 36 × 100          |
| $B$   | 17.919(3) | Radiation                        | MoK $\alpha$ /Graphite |
| $C$   | 5.292(1)  | No. of intensities               | 1007                   |
| $\beta$ (°)   | 104.05(2) | No. of unique $ F $              | 943                    |
| $V$ (Å <sup>3</sup> )                               | 899.3(3)  | No. of $ F_o  > 5\sigma_F$       | 557                    |
| Space group   | $C2/m$    | $R(\text{obs})$ %                | 2.6                    |
| $Z$   | 2         | $wR(\text{obs})$ %               | 2.6                    |
| $R = \Sigma( F_o  -  F_c )/\Sigma F_o $             |           |                                  |                        |
| $wR = [Sw( F_o  -  F_c )^2/SF_o^2]^{1/2}$ , $w = 1$ |           |                                  |                        |

**TABLE 4.** Atom positions and displacement parameters ( $\times 10^4$ ) for obertiite

|     | $x$       | $y$        | $z$       | $U_{11}$ | $U_{22}$ | $U_{33}$ | $U_{23}$ | $U_{13}$ | $U_{12}$ | $U_{eq}$ |
|-----|-----------|------------|-----------|----------|----------|----------|----------|----------|----------|----------|
| O1  | 0.1136(4) | 0.0858(2)  | 0.2176(6) | 62(18)   | 47(17)   | 91(18)   | 0(11)    | 7(15)    | 5(11)    | 68(11)   |
| O2  | 0.1170(3) | 0.1652(2)  | 0.7249(6) | 52(16)   | 128(18)  | 40(15)   | 0(12)    | 1(13)    | -7(12)   | 75(10)   |
| O3  | 0.1034(5) | 0          | 0.7061(9) | 54(23)   | 127(23)  | 43(21)   | 0        | 21(19)   | 0        | 73(14)   |
| O4  | 0.3578(4) | 0.2508(2)  | 0.7995(7) | 115(18)  | 68(15)   | 111(19)  | 12(12)   | 5(15)    | -36(12)  | 102(11)  |
| O5  | 0.3497(3) | 0.1276(2)  | 0.0805(7) | 69(14)   | 130(15)  | 75(15)   | 49(12)   | 30(12)   | -8(13)   | 89(9)    |
| O6  | 0.3461(3) | 0.1200(2)  | 0.5798(6) | 84(15)   | 105(15)  | 66(15)   | -46(12)  | 3(12)    | -1(13)   | 88(9)    |
| O7  | 0.3434(5) | 0          | 0.2996(9) | 99(22)   | 87(21)   | 138(26)  | 0        | 51(19)   | 0        | 104(14)  |
| T1  | 0.2836(2) | 0.08524(6) | 0.2941(3) | 58(6)    | 55(6)    | 50(6)    | -4(4)    | 13(5)    | 8(4)     | 54(4)    |
| T2  | 0.2883(2) | 0.17078(6) | 0.7985(3) | 51(6)    | 63(5)    | 40(5)    | 3(4)     | 1(5)     | -8(4)    | 53(3)    |
| M1A | 0         | 0.0788(2)  | 1/2       | 94(9)*   | 94(9)*   | 47(9)†   | 0        | 2(7)‡    | 0        | 81(5)§   |
| M1  | 0         | 0.0910(8)  | 1/2       | 94(9)*   | 94(9)*   | 47(9)†   | 0        | 2(7)‡    | 0        | 81(5)§   |
| M2  | 0         | 0.18172(9) | 0         | 78(9)    | 75(7)    | 72(9)    | 0        | 24(7)    | 0        | 74(5)    |
| M3  | 0         | 0          | 0         | 64(16)   | 82(15)   | 81(16)   | 0        | 7(12)    | 0        | 78(10)   |
| M4  | 0         | 0.2738(2)  | 1/2       | 240(18)  | 159(15)  | 253(19)  | 0        | 160(14)  | 0        | 200(11)  |
| Am  | 0.048(1)  | 1/2        | 0.101(2)  |          |          |          |          |          | 200      |          |
| A2  | 0         | 0.4886(8)  | 0         |          |          |          |          |          | 200      |          |

\*†‡§ These pairs are constrained to be equal.

**TABLE 5.** Selected interatomic distances ( $\text{\AA}$ ) and angles ( $^\circ$ ) in obertiite

|          |    |          |         |    |           |
|----------|----|----------|---------|----|-----------|
| T1-O1    |    | 1.612(4) | T2-O2   |    | 1.628(4)  |
| T1-O5    |    | 1.621(4) | T2-O4   |    | 1.586(3)  |
| T1-O6    |    | 1.612(3) | T2-O5   |    | 1.659(3)  |
| T1-O6    |    | 1.633(2) | T2-O6   |    | 1.675(4)  |
| <T1-O>   |    | 1.620    | <T2-O>  |    | 1.637     |
| M1-O1    | x2 | 2.071(4) | M1A-O1  | x2 | 2.069(4)  |
| M1-O2    | x2 | 2.111(4) | M1A-O2  | x2 | 1.957(10) |
| M1-O3    | x2 | 1.916(4) | M1A-O3  | x2 | 2.081(11) |
| <M1-O>   |    | 2.034    | <M1A-O> |    | 2.036     |
| M2-O1    | x2 | 2.212(3) | M3-O1   | x4 | 2.074(3)  |
| M2-O2    | x2 | 2.079(4) | M3-O3   | x2 | 2.050(5)  |
| M2-O4    | x2 | 1.951(3) | <M3-O>  |    | 2.066     |
| <M2-O>   |    | 2.081    |         |    |           |
| M4-O2    | x2 | 2.419(4) | Am-O5   | x2 | 2.984(8)  |
| M4-O4    | x2 | 2.389(4) | Am-O5'  | x2 | 2.758(8)  |
| M4-O5    | x2 | 2.936(4) | Am-O6   | x2 | 2.774(7)  |
| M4-O6    | x2 | 2.525(4) | Am-O7   |    | 2.478(13) |
| <M4-O>   |    | 2.567    | Am-O7'  |    | 2.589(14) |
| A-O5     | x4 | 2.806(3) | A2-O5   | x2 | 2.975(13) |
| A-O6     | x4 | 3.194(3) | A2-O5'  | x2 | 2.642(12) |
| A-O7     | x2 | 2.457(6) | A2-O6   | x2 | 3.336(10) |
|          |    |          | A2-O6'  | x2 | 3.060(10) |
| T1-O5-T2 |    | 136.6(2) | A2-O7   | x2 | 2.466(6)  |
| T1-O6-T2 |    | 138.0(2) |         |    |           |
| T1-O7-T1 |    | 138.5(4) | M1-M1A  |    | 0.22(1)   |

**TABLE 6.** Refined site-scattering values and assigned site-populations

|     | Refined site-scattering (epfu) | Site-population (apfu)  | Calculated site-scattering (epfu) |
|-----|--------------------------------|---|-----------------------------------|
| M1A | 28.1(7)                        | 0.86 Ti + 0.37 Mn <sup>3+</sup> (0.37 Fe <sup>3+</sup> )*   | 28.2                              |
| M1  | 8.7(4)                         | 0.77 Mg   | 9.2                               |
| M2  | 32.2(3)                        | 0.03 Al + 0.30 Fe <sup>3+</sup> + 0.35 Fe <sup>2+</sup> + 1.32 Mg (0.31 Mn <sup>2+</sup> + 0.28 Fe <sup>3+</sup> )* | 33.1                              |
| M3  | 12.0(2)                        | 1.00 Mg   | 12                                |
| M4  | 23.5(3)                        | 0.06 Fe <sup>2+</sup> + 1.84 Na + 0.08 Ca (0.06 Mn <sup>2+</sup> )*   | 23.8                              |
| Am  | 7.5(2)                         | 0.18 K + 0.38 Na  | 7.6                               |
| A2  | 4.8(2)                         | 0.44 Na   | 4.8                               |

\* Values in parentheses are those assigned for Mn = Mn<sup>2+</sup>.

### The T sites

The <T1-O> distance of 1.619  $\text{\AA}$  indicates that there is negligible Al at the T1 site. The observed scattering at T2 indicates that there is no Ti at this site (Ti does occur at T2 in Ti-rich richterite; Oberti et al. 1992).

### The M1,2,3 sites

The total refined scattering at the M1, M1A, M2, and M3 sites is 81.0(7) electrons per formula unit (epfu); the total effective scattering of the C-group cations in the formula unit of Table 1 is 82.9 epfu. These values are sufficiently close to allow us to use Table 1 as an indicator of site populations. We will omit consideration of Li and Zn as the effective scattering of these species is within the standard deviations of the refined scattering values (Table 6).

The refined site-scattering value at the M3 site is 12.0(2) epfu, indicating that this site is completely occupied by Mg. This leaves the remaining C-group cations to be assigned to the M1, M1A, and M2 sites. The M1 and M1A sites (Table 4) are displaced

relative to each other in the **b** direction along the twofold rotation axis at 0 y  $\frac{1}{2}$ . The O3 site is occupied dominantly by O<sup>2-</sup>, but also by OH + F (Table 1). Where O3 is occupied by O<sup>2-</sup>, the sum of the bond valence locally incident at O3 must be 2 v.u. (valence units); where O3 is occupied by OH or F, the sum of the bond valence incident at O3 must be 1 v.u. Here is the driving force behind the splitting (positional disorder) at the M1 and M1A sites: where O3 = O<sup>2-</sup>, the M1A site is occupied by a high-valence cation (Ti<sup>4+</sup> and possibly Mn<sup>3+</sup> or Fe<sup>3+</sup>) and this cation is displaced toward the O3 site to maximize the bond valence incident at O3; where O3 = OH or F, the M1 site is occupied by a divalent cation, as is generally the case in amphiboles. Thus we tentatively assign Ti<sup>4+</sup> and (Mn<sup>3+</sup> + Fe<sup>3+</sup>) or Fe<sup>3+</sup> to the M1A site.

Initial site-populations for the M2 site were derived by subtracting the assigned M1, M1A and M3 site-populations from the initial unit formula. For the model with Mn<sup>3+</sup> present, the Fe<sup>2+</sup>/Fe<sup>3+</sup> ratio was adjusted to bring the <M2-O> distance calculated from the equation of Hawthorne (1983) into agreement with the observed <M2-O> distance and the unit formula was recalculated. One additional cycle of this procedure resulted in self-consistency.

### The M4 site

The C-group cations in excess of 5.0 atoms per formula unit (apfu) were assigned to M4, together with the Ca indicated by the unit formula and sufficient Na to fill the site.

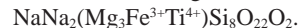
### The A sites

The Am and A2 sites both show significant electron density (Table 6). From the detailed work of Hawthorne et al. (1996) on A-site stereochemistry in monoclinic amphiboles, we may assign Na to the A2 site and a mixture of K and Na to the Am site, taking the K content of Am from the unit formula of Table 1.

The final site-populations are given in Table 6. There is reasonably good agreement between the refined site-scattering values and those calculated from the assigned site-populations.

### The end-member formula of obertiite

The unit formula of Table 1 may be simplified by filling each of the sites in the structure by the dominant constituent species: T1 = T2 = Si, M1 = Mg, M1A = Ti<sup>4+</sup>, M2 = Mg + Fe<sup>3+</sup> + Mn<sup>3+</sup> + Fe<sup>2+</sup>, M3 = Mg, M4 = Na, A = Na, O3 = O. This results in the following ideal end-member formula for obertiite



Obertiite is the second ideally anhydrous amphibole described, the other being ungarettiite,  $\text{NaNa}_2(\text{Mn}_3^{3+}\text{Mn}_2^{2+})\text{Si}_8\text{O}_{22}\text{O}_2$ .

Obertiite may be formally derived from magnesiobarfvedsonite,  $\text{NaNa}_2(\text{Mg}_4\text{Fe}^{3+})\text{Si}_8\text{O}_{22}(\text{OH})_2$ , by the substitution  $\text{M}^{\text{IA}}\text{Ti}^{4+} + \text{H}^{\square} \rightarrow \text{M}^{\text{I}}\text{Mg} + \text{H}^{\text{H}_2}$ .

### Local order in obertiite

Hawthorne (1997) has shown how local bond-valence constraints exert stringent controls on short-range order in amphiboles. The case of obertiite is particularly interesting as it involves disorder of (OH,F) and O<sup>2-</sup> at the same crystallographic site and, in this regard, is similar to the situation in tourmaline (Hawthorne 1996; Taylor et al. 1995).

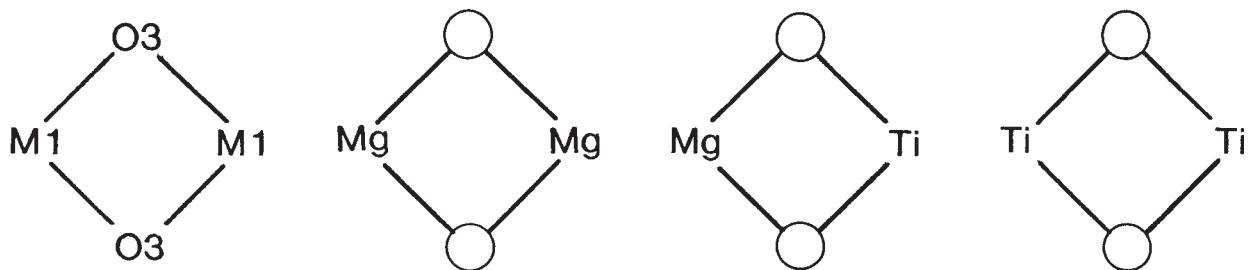


FIGURE 1. Possible local configurations around the O3 sites in end-member obertiite; the O3 sites (unshaded circles) are always occupied by O<sup>2-</sup>.

|  |         |         |
|--|---------|---------|
|  | 0.28 vu | 0.28 vu |
|  | —       | 0.58    |
|  | 0.20    | —       |
|  | 0.29    | —       |
|  | 0.23    | 0.23    |

FIGURE 2. Possible local configurations around the O3 sites in obertiite; the O3 sites can be occupied by O<sup>2-</sup> or (OH,F). Possible amounts of local configurations compatible with the bulk composition of Table 1 are shown. The unshaded circles are O<sup>2-</sup>, the unshaded double circles are (OH,F).

The O3 site is surrounded by two M1 and one M3 sites in obertiite, M3 = Mg, and hence local variation in O3 occupancy must couple to local variation in M1 occupancy. It is instructive first to consider the situation in the end-member composition (Fig. 1). The local pairs of M1 sites linked to a pair of O3 sites may be occupied by MgMg, MgTi or TiTi. Both O3 sites in Figure 1 are occupied by O<sup>2-</sup>, and hence the local bond-valence requirements of O<sup>2-</sup> at O3 preclude the local configuration MgMg. This being the case, the stoichiometry precludes the local configuration TiTi, and hence the local configuration in the end-member must be MgTi.

The situation in obertiite is more complicated, as there are additional cations present at M1A (Mn<sup>3+</sup>) and anions at O3 (OH,F). However, there is the constraint that, in the end-member, the pair MgTi satisfies the local bond-valence requirements of O<sup>2-</sup> at the O3 site. Moreover, we know that, in ungarettiite, the pair Mn<sup>3+</sup>Mn<sup>3+</sup> satisfies the local bond-valence requirements of O<sup>2-</sup> at O3. This suggests the local configurations indicated in Figure 2: MgTi<sup>4+</sup>, Mn<sup>3+</sup>Mn<sup>3+</sup>, and Ti<sup>4+</sup>Ti<sup>4+</sup> linked to O<sup>2-</sup> at O3, and MgMg linked to (OH,F) at O3. Alternatively, MgTi and Mn<sup>3+</sup>Ti or Fe<sup>3+</sup>Ti could link to O<sup>2-</sup> at O3, and MgMg link to (OH,F) at O3. The stoichiometry allows both end-member models for short-range arrangements.

#### ACKNOWLEDGMENTS

We thank André Lalonde and Lee Groat for their reviews of this manuscript, and Rodney Lee of Simkev Minerals for his help in acquiring this mineral. This work was supported by Natural Sciences and Engineering Research Council of Canada grants to F.C.H.

#### REFERENCES CITED

- Appleman, D.E. and Evans, H.T. Jr. (1973) Job 9214: Indexing and least-squares refinement of powder diffraction data. U.S. National Technical Information Service, Document PB 216 188.
- Hawthorne, F.C. (1983) The crystal chemistry of the amphiboles. Canadian Mineralogist, 21, 173–480.
- (1996) Structural mechanisms for light-element variations in tourmaline. Canadian Mineralogist, 34, 123–132.
- (1997) Short-range order in amphiboles: a bond-valence approach. Canadian Mineralogist, 35, 203–216.
- Hawthorne, F.C. and Groat, L.A. (1985) The crystal structure of wroewolfeite, a mineral with [Cu<sub>4</sub>(OH)<sub>6</sub>(SO<sub>4</sub>)<sub>2</sub>(H<sub>2</sub>O)] sheets. American Mineralogist, 70, 1050–1055.
- Hawthorne, F.C. and Grundy, H.D. (1976) The crystal chemistry of the amphiboles. IV. X-ray and neutron refinements of the crystal structure of tremolite. Canadian Mineralogist, 14, 334–345.
- Hawthorne, F.C., Ungaretti, L., Oberti, R., Bottazzi, P., and Czamanske, G.K. (1993) Li: An important component in igneous alkali amphiboles. American Mineralogist, 78, 733–745.
- Hawthorne, F.C., Oberti, R., Cannillo, E., Sardone, N., Zanetti, A., Grice, J.D., and Ashley, P.M. (1995) A new anhydrous amphibole from the Hoskins mine, Grenfell, New South Wales, Australia: Description and crystal structure of ungarettiite, Na<sub>2</sub>Na<sub>2</sub>(Mn<sup>2+</sup>Mn<sup>3+</sup>)Si<sub>8</sub>O<sub>22</sub>O<sub>2</sub>. American Mineralogist, 80, 165–172.

- Hawthorne, F.C., Oberti, R., and Sardone, N., (1996) Sodium at the A site in clinoamphiboles: the effects of composition on patterns of order. *Canadian Mineralogist*, 34, 577–593.
- Hentschel, G. (1975) Die Mineralfen der basaltischen Gesteine im Laacher Vulkangebeit. *Der Aufschluss*, 26, 65–87.
- (1977) Selected minerals from the volcanic district of Laacher See, Germany. *Mineralogical Record*, 8, 313–326.
- Oberti, R., Ungaretti, L., Cannillo, E., and Hawthorne, F.C. (1992) The behaviour of Ti in amphiboles. I. Four- and six-coordinate Ti in richterite. *European Journal of Mineralogy*, 3, 425–439.
- Ottolini, L., Bottazzi, P., and Vannucci, R. (1993) Quantification of lithium, beryllium and boron in silicates by secondary ion mass spectrometry using conventional energy filtering. *Analytical Chemistry*, 65, 1960–1968.
- Ottolini, L., Bottazzi, P., Zanetti, A., and Vannucci, R. (1995) Determination of hydrogen in silicates by Secondary Ion Mass Spectrometry. *The Analyst*, 120, 1309–1313.
- Pouchou, J.L. and Pichoir, F. (1984) A new model for quantitative analysis: Part I. Application to the analysis of homogeneous samples. *La Recherche Aerospatiale*, 3, 13–38.
- Pouchou, J.L. and Pichoir, F. (1985) 'PAP'  $\phi(pZ)$  procedure for improved quantitative microanalysis, p. 104–160. *Microbeam analysis–1985*. San Francisco Press, San Francisco.
- Shannon, R.D. (1976) Revised effective ionic radii and systematic studies of interatomic distances in halides and chalcogenides. *Acta Crystallographica*, A32, 751–767.
- Taylor, M.C., Cooper, M.A., and Hawthorne, F.C. (1995) Local charge-compensation in hydroxyl-deficient uvite. *Canadian Mineralogist*, 33, 1215–1221.

MANUSCRIPT RECEIVED DECEMBER 18, 1998

MANUSCRIPT ACCEPTED AUGUST 9, 1999

PAPER HANDLED BY LEE A. GROAT